npj | heritage science

Article

https://doi.org/10.1038/s40494-026-02307-y

Analyzing the surface black discoloration of oracle plastrons from the Taijiasi Site, China

Check for updates

Juan Yang[1], Decai Gong[1], Pujun Jin[2], Xiaolin He[3] & Zhengquan Yao[4] ✉

Several Shang and Zhou Dynasty oracle plastrons from the Taijiasi Site (Funan, Anhui, China) exhibit random flake- or patch-like surface black deposits unlikely induced by burning or pyromancy. Scanning electron microscopy-energy dispersive X-ray spectroscopy (SEM-EDS) and X-ray photoelectron spectroscopy (XPS) identified the elements causing the black color as Fe and Mn. The chromogenic mechanisms were explored via micro-X-ray fluorescence spectroscopy (μ-XRF) mapping analysis of the distribution of Fe, Mn, Al, etc. The Fe ions likely existed as trivalent oxide precipitates and Mn^{4+} in its typical coordination mode in oxides. Thus, the black discoloration resulted from the enriched Mn and Fe, oxidation-reduction reactions, and microbial activities in the burial environment. Colloidal form Mn^{4+} and Fe^{3+} adsorbed on the plastron surface and complexed with humic acids from organic matter degradation to significantly darken the color. The results could effectively support the research, conservation, and restoration of oracle plastrons.

Inscribed turtle shells (plastrons and, less often, carapaces) and animal bones used for divination in the Shang and Zhou Dynasties are collectively known as oracle bones[1], which are invaluable cultural relics unique to China. Since epigrapher Wang Yirong in Beijing first identified oracle bones as important antiquities in 1899[2], diversified studies on oracle bones[3] commenced. Over the years, archaeological excavations have unearthed oracle bones in many places across China. The discovery of several of these sites is of particular significance: From the Yinxu Site[4] in Anyang, Henan Province, recognized as the capital of the late Shang Dynasty, archaeologists unearthed the largest number of oracle bones, which directly confirmed the historical existence of the Shang Dynasty. Meanwhile, the inscriptions on the oracle bones form the key basis for exploring the origins of Chinese characters[5]. The Zhouyuan Site in Shaanxi is the core discovery site of Western Zhou Dynasty oracle bones[6,7], whose preparation, drilling, and chiseling processes differed significantly from those of the Shang Dynasty. Those oracle bones provided indispensable empirical evidence for studying the early Zhou history[8]. The Daxinzhuang Site in Jinan, Shandong Province, is currently the only Shang Dynasty oracle bone site other than the Yinxu Site, and the unearthed oracle bones shared the inscription style of those from the Yinxu Site but featured drilling and chiseling patterns with distinct local characteristics[9]. In recent years, a large number of oracle bones have been unearthed from various Shang and Zhou Dynasty sites discovered in Anhui[10–13], of which the Taijiasi Site in Funan is the most representative.

The Taijiasi Site is a significant Shang and Zhou Dynasty archaeological site in the middle Huai River Basin, as shown in Fig. 1, whose main period of occupation dates to the Shang Dynasty. From 2014 to 2017, a joint archaeological excavation by the Anhui Provincial Institute of Cultural Relics and Archaeology and Wuhan University uncovered abundant relics at the site, including pottery, pottery molds, bronze ware, animal bones, and oracle plastrons[10]. Among them, a large number of oracle turtle shells were found with traces of usage but no inscription on their surfaces. Their preparation, drilling, chiseling, and pyro-plastromancy characteristics are consistent with those unearthed at the Huanbei Shang Dynasty City Site in the northern part of central China, making them valuable materials for exploring the plastromancy methods in the middle Shang Dynasty and the spiritual world reflected.

Interestingly, we noticed black discoloration on most of the surface of the oracle plastrons unearthed at the Taijiasi Site. Such discoloration affects the authenticity and appearance of the oracle plastrons and, to some extent, hinders the scientific observation of the traces of oracle plastron preparation. In addition, its impact on the long-term preservation of oracle plastrons merits investigation.

The black discoloration on the surfaces of oracle plastrons unearthed at Taijiasi Site can be roughly divided into three types: The first type is the black burn marks produced by pyro-plastromancy, which are found along the edge and/or at the bottom of the drill (chisel)

[1]Department of History of Science and Scientific Archaeology, University of Science and Technology of China, Hefei, Anhui, China. [2]School of Materials Science and Engineering, Shaanxi Normal University, Xi'an, Shaanxi, China. [3]School of History, Wuhan University, Wuhan, Hubei, China. [4]Anhui Provincial Institute of Cultural Relics and Archaeology, Hefei, Anhui, China. ✉e-mail: 20597220@qq.com

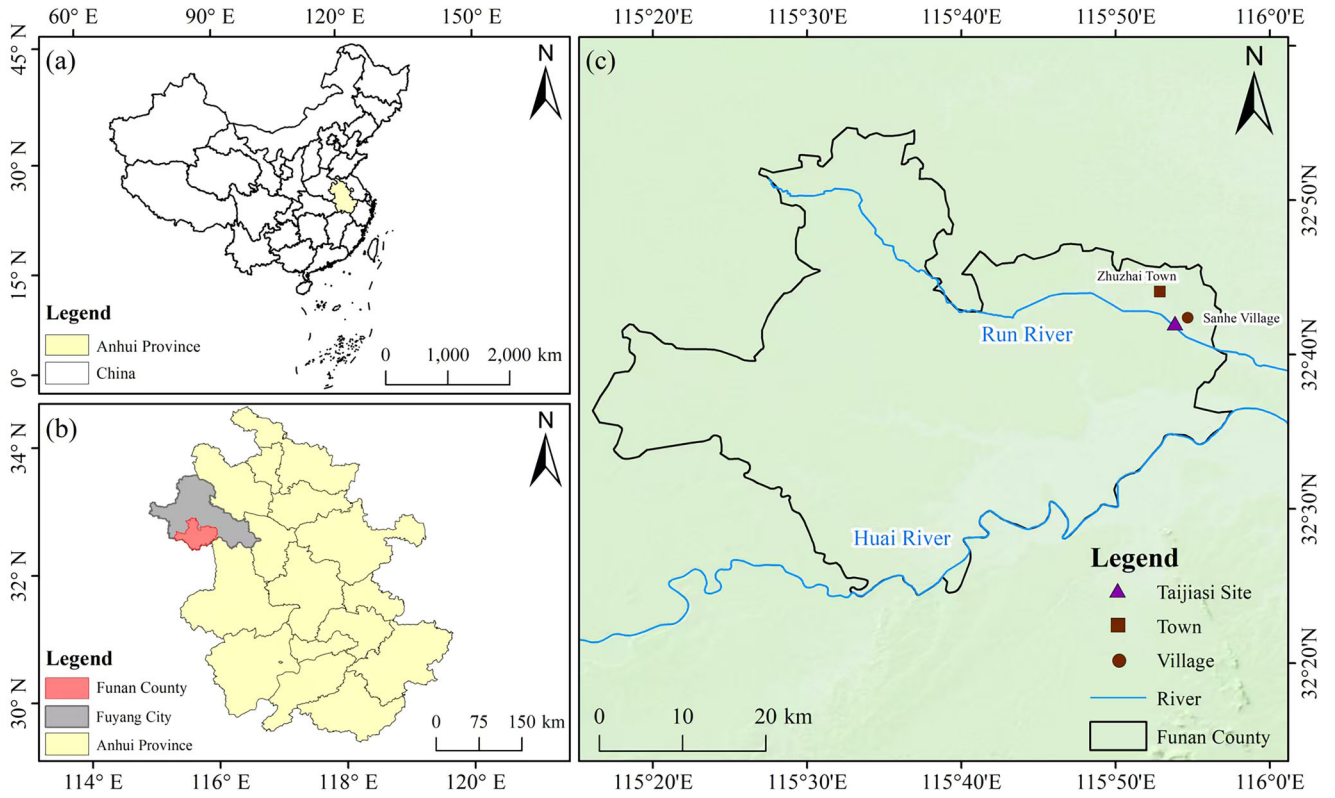

Fig. 1 | Geographic location of the Taijiasi Site. a Geographic location of Anhui Province in China; **b** Geographic location of Funan County and Fuyang City in Anhui Province; **c** Geographic location of Taijiasi Site in Funan County.

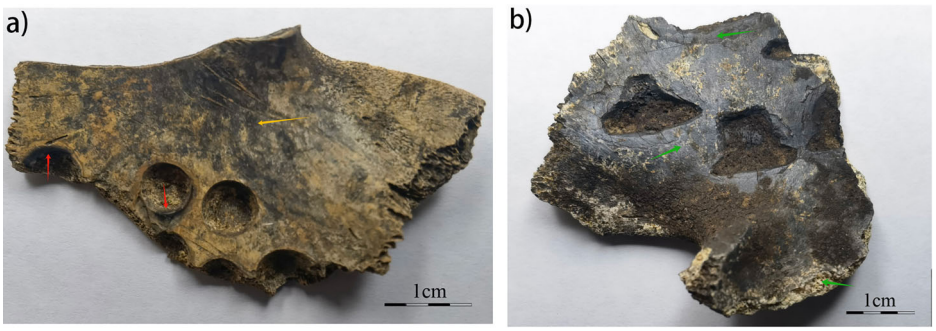

Fig. 2 | Black discoloration of turtle plastrons unearthed at the Taijiasi Site. a Black burn marks produced by pyro-plastromancy and black deposits on the sample H33:1-007. **b** Burning marks on the sample H233:3-001.

holes, as shown in Fig. 2a. The scorched area takes on a darker black color due to carbonization, naturally attributing to the heated carbonization during pyro-plastromancy[14]. The second type is often the result of burning part of or the whole plastron. As indicated by the green arrow in Fig. 2b, a clear black scorched surface can be observed, even with a local grayish-white color due to overheating, which is often the result of burning after discarding (or storing). The third type is black deposits randomly distributed as flakes or patches on the surface of the oracle plastrons, with uneven coloration, as indicated by the yellow arrow in Fig. 2a. The formation of such black substance is apparently not related to the burning or pyro-plastromancy process but to the burial environment. Previous research has reported on the discoloration of cultural relics due to buried environmental factors. Testing and analysis of the black cementation on the surface of bone fossil excavated at the Bailongdong Site in Hubei Province revealed that the chromogenic phases are mainly paragenic deposits of siderite, hematite, and $Fe_{25}(PO_4)_{14}(OH)_{24}$, which are related to CO_3^{2-} and Fe ions in the burial environment[15]. The discoloration of wooden artifacts found in marine wrecks has been linked to the metabolic activities of iron-sulfur bacteria in the preservation environment[16,17]. The mechanism of the discoloration of the turtle plastrons remained unclear. Whether the black deposits on the oracle plastron surface relate to the microbial activities in the burial environment or whether the porous structure of the oracle plastron resulting from the organic matter loss to the burial environment absorbed minerals and carbon from the soil to form the black color warrants research attention. To this end, this study employed various analysis and detection methods to characterize the morphological structure and chemical composition of the black deposits on the surface of the oracle plastrons unearthed from the Taijiasi Site and explored their formation mechanisms.

Methods

Experimental sample

Two representative samples were selected for analysis in this study: H253:2-014 and H338:2-001, as shown in Fig. 3. Both samples are poorly preserved, with large areas of black deposits on their surface, which are planar and

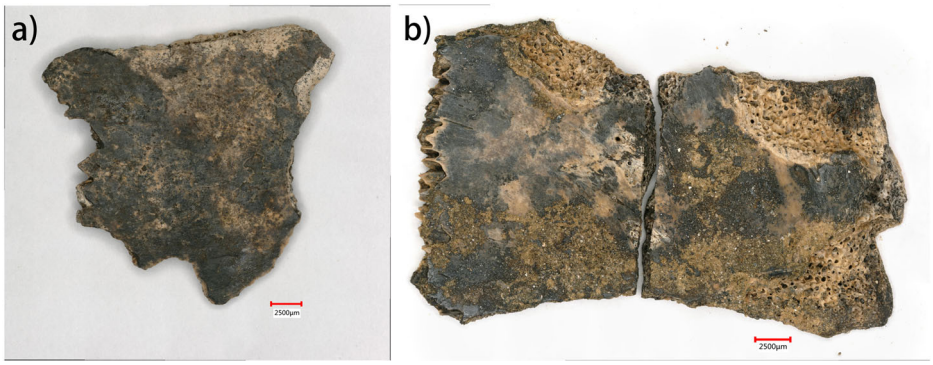

Fig. 3 | Samples of the oracle plastrons unearthed from the Taijiasi Site. a Sample H253:2-014. **b** Sample H338:2-001.

smooth without bulging. Other than the black deposits, varying degrees of contaminant attachment are also observed on the oracle plastron surface. The black deposits on the surfaces of the two samples are extensively distributed, covering almost the entire oracle plastron surface.

Experimental methods

SEM-EDS (scanning electron microscopy with energy dispersive X-ray spectroscopy). The microscopic morphology and elemental distribution of the oracle plastron samples were observed and studied using an FEI Quanta 200 environmental scanning electron microscope (SEM) operating in the high vacuum mode at 6×10^{-3} Pa, with an acceleration voltage of 20 kV and gold spraying on the sample surface.

Laser confocal microscopy. A Keyence VK-X250K laser scanning confocal microscope was used to observe the 2D and 3D morphology of the oracle plastrons with a 108 nm laser source. The VK-X serious multi-file analysis software was used for roughness analysis.

X-ray photoelectron spectroscopy. The chemical state of the oracle plastron samples was analyzed using a Thermo Fisher EscaLab Xi+ X-ray photoelectron spectrometer (XPS), with an energy scanning range of 0–5000 eV.

X-ray fluorescence spectrometry. A Shimadzu EDX-7000 energy-dispersive X-ray fluorescence spectrometer (ED-XRF) was used for non-destructive elemental content analysis of the oracle plastron samples. The elemental analysis range spanned from 11 (Na) to 92 (U), the tube voltage was 50 kV, and the tube current was 1000 μA. A 1 mm collimator was used for analysis, and a Mylar film covered the sample surface.

Micro-X-ray fluorescence spectroscopy. The content and distribution of Al, Fe, and Mn in the oracle plastron samples were non-destructively detected by mapping analysis using a Bruker M4 Tornado Micro-X-ray fluorescence spectrometer (μ-XRF) equipped with a rhodium target, a multi-conducting capillary, and a vacuum optical path. The operating voltage was 50 kV, and the operating current was 600 μA. The scanning step size was 15 μm.

Results

Oracle plastron morphology observation

Generally, a turtle's plastron consists of three layers: the outermost horny shield (typically absent in unearthed oracle plastrons, as it was removed during preparation), a middle compact bone layer, and an innermost cancellous bone layer. Figure 4 shows the morphology of the H253:2-014 oracle plastron sample under scanning electron microscopy (SEM). Loose pore-like structures and fiber-like structures can be observed in the samples. The pore-like structures are mainly irregularly circular and elliptical, and the maximum pore diameter is about 27 μm. Previous studies have shown that fresh oracle plastrons are primarily composed of both inorganic and organic components. The inorganic material forms a porous network that serves as the structural scaffold, while the organic substances act as binders, filling and reinforcing this framework. Microscopic analysis reveals a well-defined three-dimensional porous architecture on the surface of these plastrons[18]. However, over time, particularly after prolonged burial, significant degradation of the organic matter occurs, leaving behind an inorganic matrix as the dominant structural framework. This transformation leads to the formation of numerous additional pores, significantly altering the original microstructure.

Figure 5 presents the 2D and 3D structures of the black deposits on the sample surface under a laser confocal microscope. The black deposits on the surface of the H253:2-014 oracle plastron sample are relatively flat, with pores of different sizes produced by organic matter loss. The H338:2-001 oracle plastron sample with contaminant particles on its black surface exhibits increased surface roughness.

Composition analysis of the black deposits and the relatively light-colored oracle plastron substrate

The compositions of oracle plastron samples were analyzed via SEM-EDS and X-ray fluorescence (XRF) spectrometry, respectively. SEM-EDS analysis (Figs. 6, 7) shows the morphology images and corresponding EDS spectra of the black deposits and the relatively light-colored substrate of two oracle plastron samples. Table 1 shows high C, O, Ca, and P contents of the black deposits and the substrate. The Ca and O contents are relatively high, both at about 30%, followed by the P and C contents, both at around 15%. The black deposits and the substrate exhibited significantly different elemental compositions in the two oracle plastron samples. The Ca content of H253:2-014 was higher in the substrate (35.61%) and lower in the black deposits (24.36%), and the Ca content of H338:2-001 was also higher in the substrate (30.84%) and lower in the black deposits (24.33%), suggesting Ca loss in the black deposits. The black deposits and substrate of the oracle plastron sample H253:2-014 contained C, O, Ca, P, Mn, and Al, while the black deposits contained additional Na, Mg, Si, K, and Mn. The black deposits and substrate of the oracle plastron sample H338:2-001 contained C, O, Ca, P, Mn, Mg, Al, and Si, while the black deposits contained additional K, Mn, and Fe. Mn and Fe were not detected in the substrates of the two oracle plastron samples, while the Mn content in the black deposits of the oracle plastron sample H253:2-014 reached 1.44%. The absence of Fe content in the black deposits of the sample H253:2-014 could be due to surface heterogeneity or the target element not being present within the micro-analytical area, resulting in the measured concentration at that point falling below the detection limit. The black deposits of the oracle plastron sample H338:2-001 showed high Mn and Fe contents of 1.5% and 5.09%, respectively. Table 2 presents the X-ray fluorescence (XRF) detection data. As shown in the table, Ca is the dominant element, accounting for approximately 70%, followed by P, which constitutes around 20%. Notable differences in elemental concentrations and Ca:P ratios are observed between Tables 1 and 2. Since two separate testing institutions were

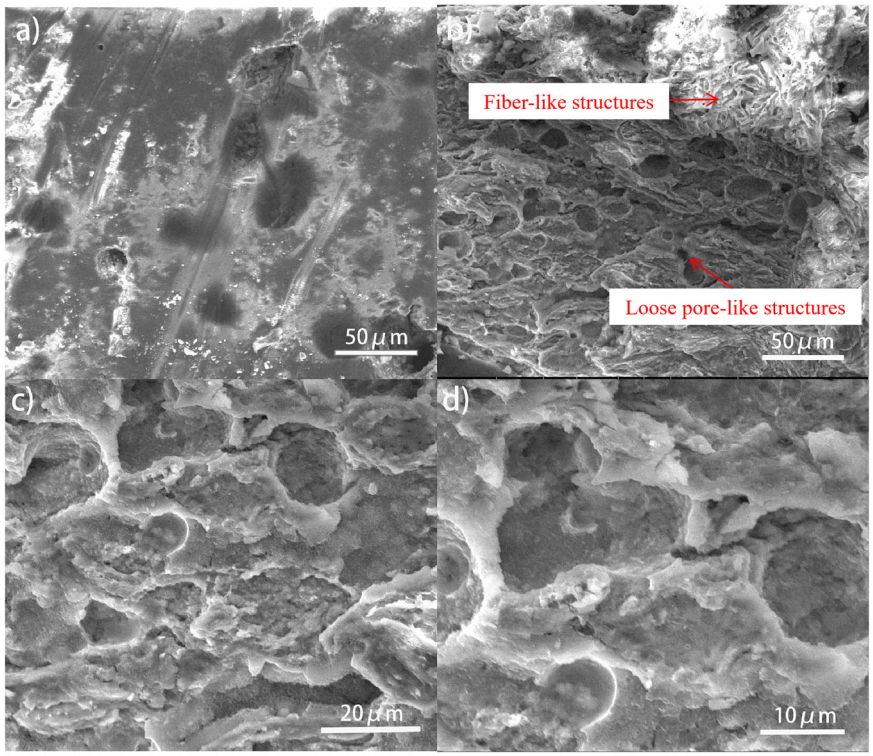

Fig. 4 | SEM images of the oracle plastron samples. **a** 1000× magnification view; **b**1000× magnification view showing fibre-like structures and loose pore-like structures; **c** 3000×magnification view; **d** 5000× magnification view.

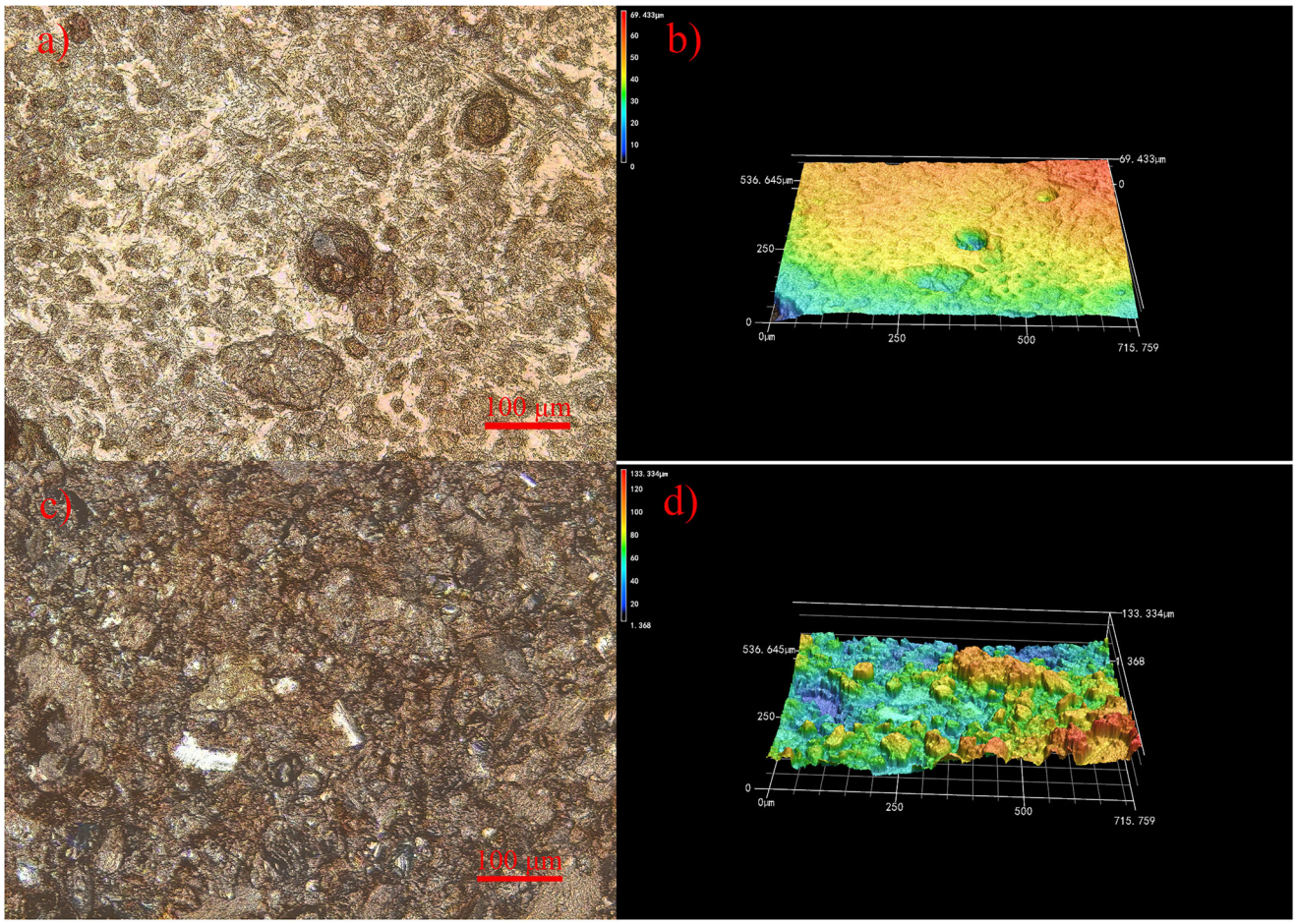

Fig. 5 | Laser confocal microscope observation of the black deposits on the oracle plastron surface. a 2D structure of the sample H253:2-014; **b** 3D structure of the sample H253:2-014; **c** 2D structure of the sample H338:2-001; **d** 3D structure of the sample H338:2-001.

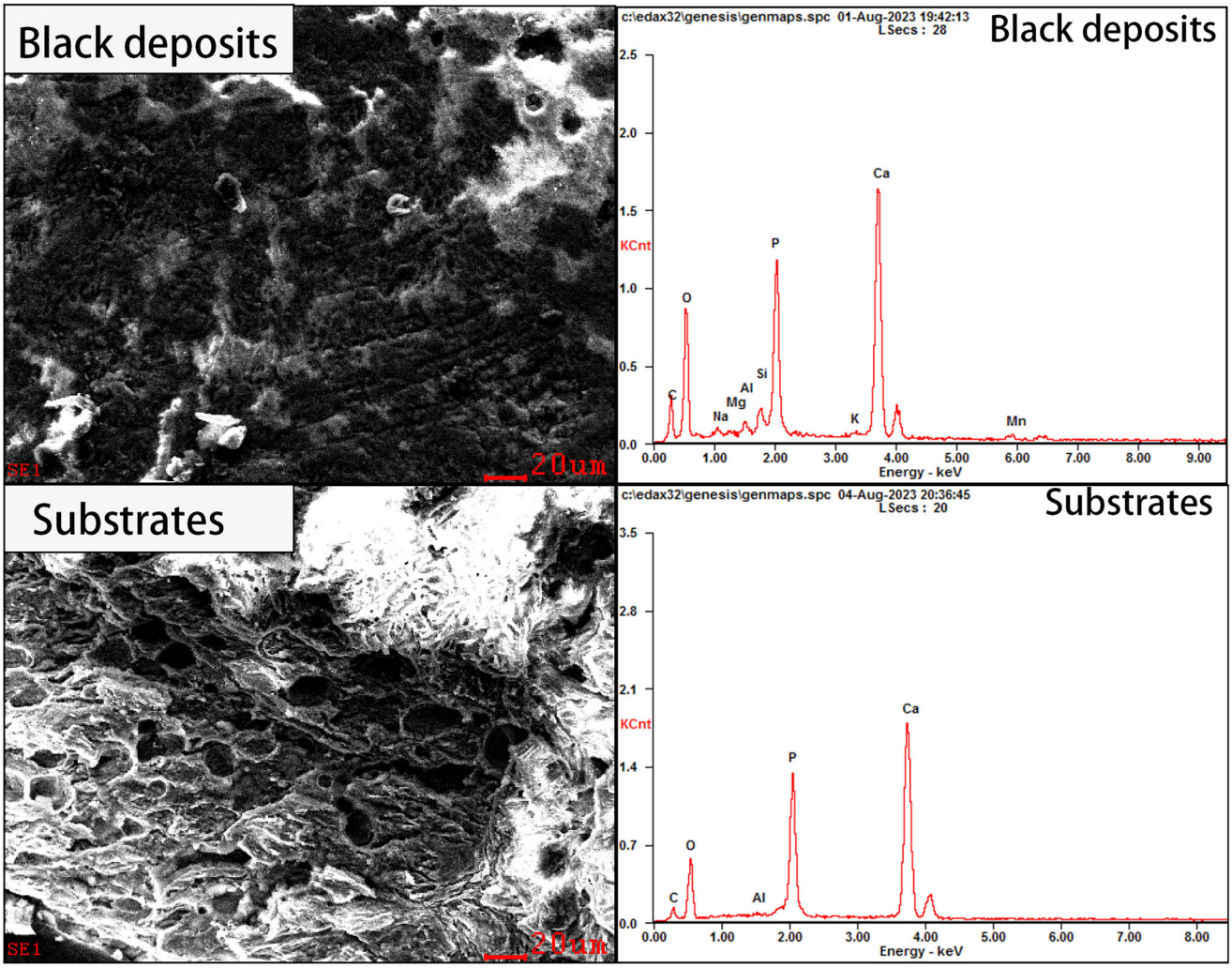

Fig. 6 | SEM-EDS analysis of the black deposits and substrates of sample H253:2-014.

commissioned to perform SEM-EDS analysis and XRF analysis respectively, discrepancies exist in the elemental compositions reported by the two institutions. The inconsistency in the selection of element types for testing has led to variations in elemental contents. Among other metallic elements, Fe and Mn exhibit relatively high concentrations, consistent with SEM-EDS data. Thus, it can be inferred that the chromogenic elements in the black deposits should be compounds of Fe and Mn.

In order to get a better understanding of the element distribution, the elemental composition characteristics of the samples were further explored by mapping analysis using μ-XRF with a multi-conducting capillary. Figure 8, 9 show the elemental mapping characteristics of Al, Fe, and Mn in the H253:2-014 and H338:2-001 samples. It can be observed that Al is dispersed in the black deposits of H253:2-014. Its source may be clay minerals, probably due to the adsorption or penetration of clay minerals on the plastron surface, consistent with the relatively uniform distribution of Al in the black deposits of H338:2-001. Mn exhibits significant enrichment in the black deposits of both samples, and its distribution range is highly consistent with that of the black deposits. H338:2-001 shows particularly pronounced local Mn enrichment in the black deposits, possibly due to the dark oxide deposition involving groundwater in the burial environment. Therefore, the formation of black deposits on the oracle plastron surface was most likely due to Mn enrichment and oxidation reaction in the burial environment. The black deposits of the two samples also show partial Fe enrichment, but this feature is not obvious. Further experiments are needed to explore the causes of such black deposits.

The chromogenic mechanisms of Mn and Fe elements in the black deposits of the turtle plastrons were further explored via XPS analysis. XPS applies to the chemical state analysis of trace elements on the surface of cultural relics. It employs X-ray photons to excite the inner electrons of the atoms on the material surface and derives the corresponding energy spectrum by energy analysis of these electrons. In addition to elemental composition detection of solid surfaces, XPS provides information on the valence state and chemical structure of the elements. Thus, it can provide further important references for understanding the composition of the black deposits on the oracle plastron surface. Figure 10 presents the XPS spectra of the two samples, where elements such as C, O, Si, Al, N, Mg, Ca, S, Fe, and Mn are detected (Table 3).

Peak deconvolution and curve-fitting analysis of the Fe 2p3/2 spectra (Fig. 11) indicate that the Fe 2p3/2 spectra of the two samples can be deconvolved into two main peaks, and their binding energies are at 711.8 eV and 713.8 eV, respectively. Thus, Fe exists in the samples in the Fe^{3+} valence state. The peak near the binding energy of 711.8 eV corresponds to Fe^{3+}, while the peak near 713.8 eV may be ascribed to binding energy displacement caused by higher oxidation state or coordination environment differences[19,20]. The peak at the binding energy of 643 eV is consistent with the Mn^{4+} characteristic peak[21]. Based on the XPS full spectrum analysis, it is speculated that Fe^{3+} may exist in an oxygen- or sulfur-containing chemical environment, while Mn^{4+} is likely to exist in its typical coordination mode in oxides.

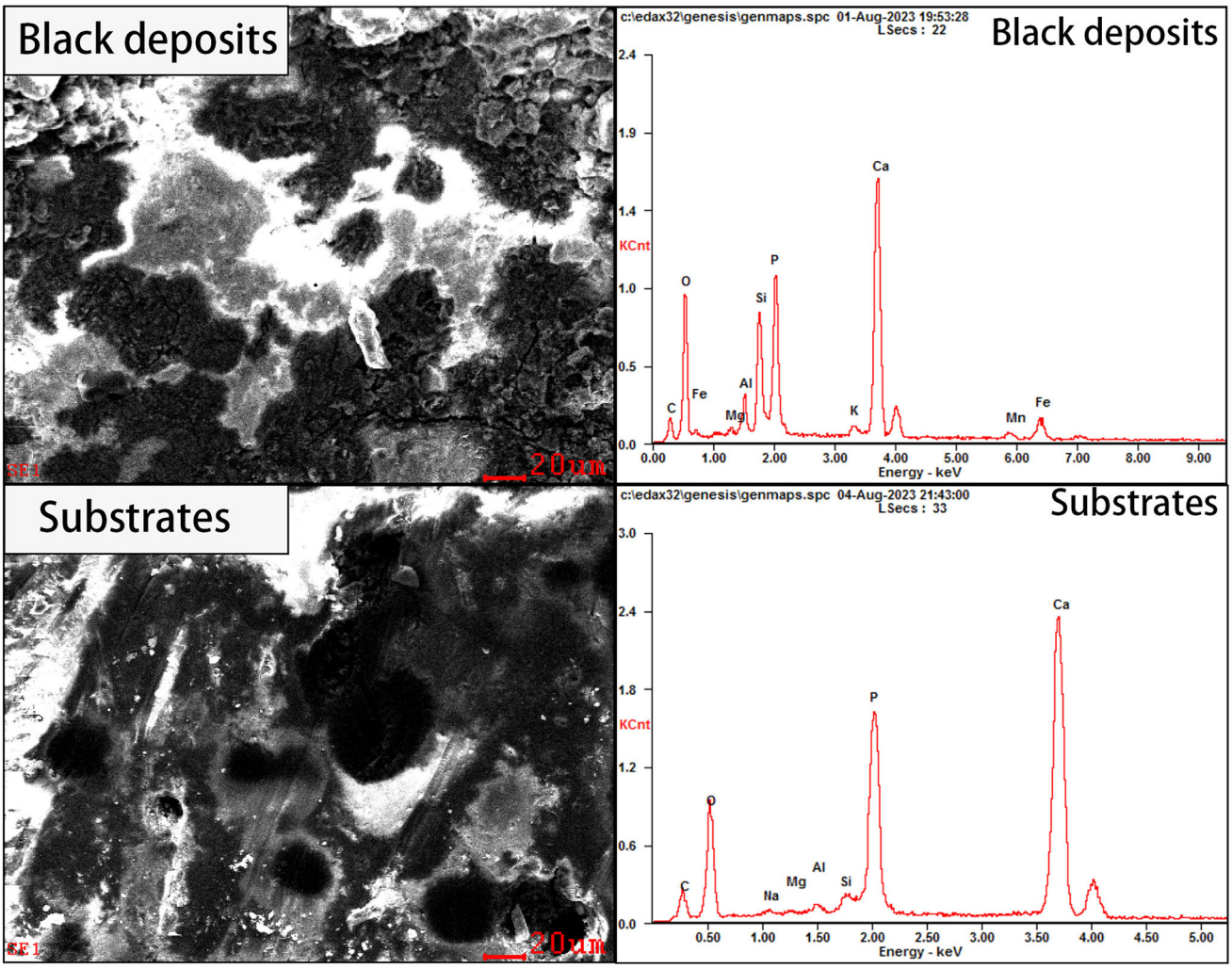

Fig. 7 | SEM-EDS analysis of the black deposits and substrates of sample H338:2-001.

Table 1 | SEM-EDS spectra-based compositional analysis results (wt%)

Sample/Element	C	O	Na	Mg	Al	Si	P	K	Ca	Mn	Fe
H253:2-014 (black deposits)	18.39	40.26	0.77	0.36	0.75	1.67	11.5	0.49	24.36	1.44	/
H253:2-014 (substrate)	9.59	38.42	/	/	0.14	/	16.24	/	35.61	/	/
H338:2-001 (black deposits)	10.7	37.76	/	0.45	1.94	6.73	10.54	0.97	24.33	1.5	5.09
H338:2-001 (substrate)	14.67	38.18	0.56	0.18	0.52	1.11	13.93	/	30.84	/	/

The detection limit is 0.01 wt%. Contents below the detection limit (e.g., Na <0.01 wt%) are omitted.

Table 2 | ED-XRF spectra-based compositional analysis results (wt%) of the oracle plastron samples.

Sample\Element	Fe	Si	Ca	Mn	Zn	P	K	Ba	S	Cu	Sr
H253:2-014	2.506	6.268	67.665	4.210	0.156	17.714	0.577	0.289	0.112	0.038	0.136
H338:2-001	0.643	/	74.211	3.312	0.068	21.091	/	0.417	0.022	0.034	0.174

Discussion

Mn^{4+} and Fe^{3+} were found in the oracle plastrons unearthed at the Taijiasi Site and their surface black deposits. The main soil types in Funan County are lime concretion black soil (48.7% of the total area) and fluvio-aquic soil (28.9%)[22]. In fluvio-aquic soil, the Mn content is 183 ± 7.3 ppm and Fe is approximately 9.12 ppm; in lime concretion black soil, Mn reaches 188 ± 9.3 ppm, whereas Fe is about 12.04 ppm[23,24]. Located north of the Yangtze River, the lime concretion black soil and fluvio-aquic soil at the Taijiasi Site are neutral and slightly alkaline[25]. The Fe content in the soil is high enough to rank among the major elements. Generally, Fe in soil exists

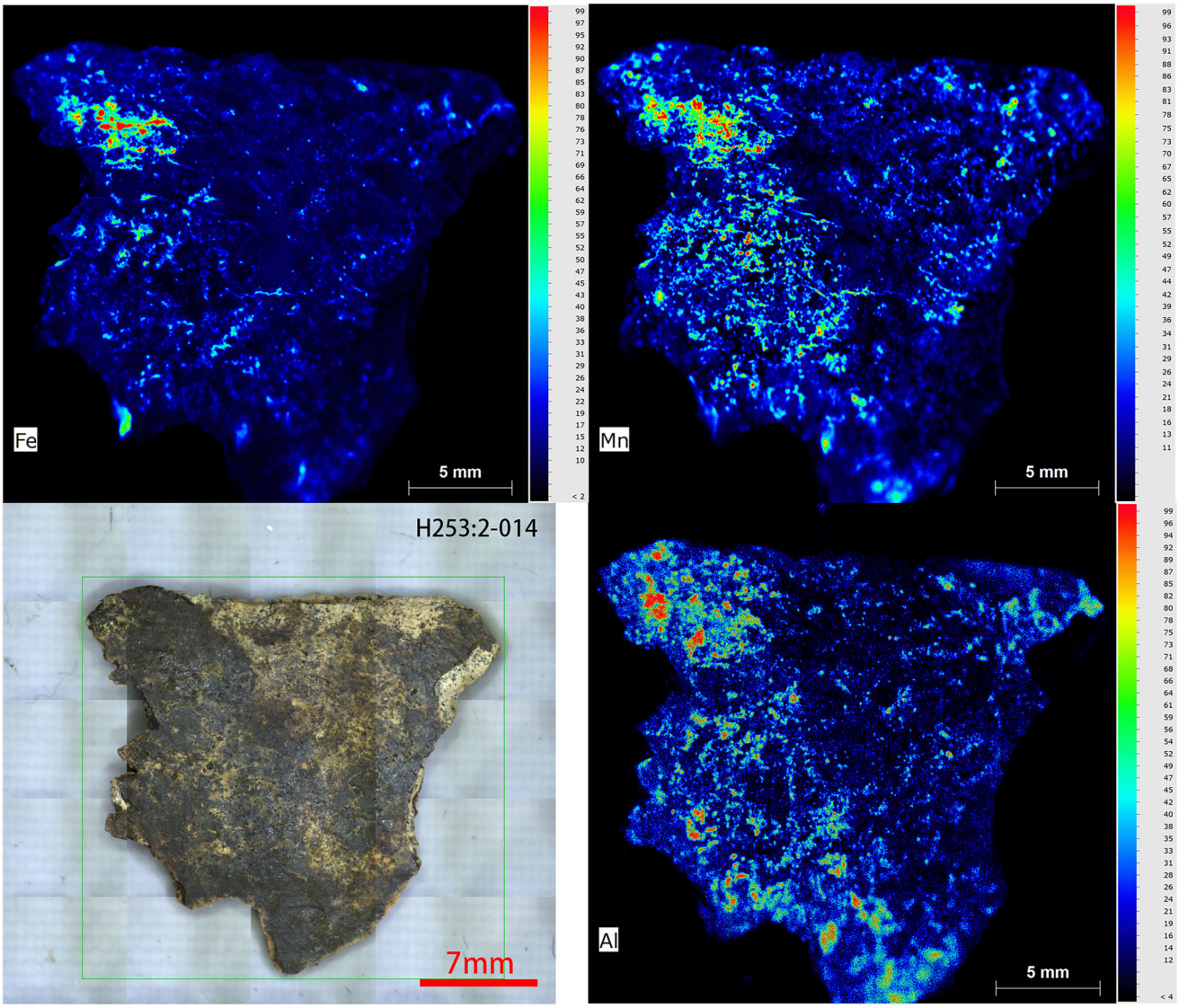

Fig. 8 | Mapping analysis results of Al, Fe, and Mn in the H253:2-014 sample.

as Fe^{3+} and Fe^{2+} in ion or compound forms. In neutral and calcareous soils, Fe mostly precipitates as a Fe^{3+} oxide[26]. With oxygen permeation, the potential Fe^{2+} in the sample can also be oxidized to Fe^{3+} by autotrophic bacteria (iron bacteria). Gothite (α-FeOOH) and hematite (Fe_2O_3) are relatively common iron oxide minerals in the soil[27]. These facts are consistent with the XPS analysis results that Fe exists mainly in trivalent and higher valence states. Mn is also a common element in soil[28], and the Mn contents in lime concretion black soil and fluvio-aquic soil are generally high[26]. Mn often migrates and accumulates extensively during soil supergene processes, forming ferromanganese nodules with Fe[29]. The potential Mn^{2+} in soil can form stable oxides such as birnessite (δ-MnO_2) by manganese oxidizing bacteria catalysis or direct air oxidation[30,31], which is consistent with the XPS analysis results that Mn exists stably as Mn^{4+}. Such oxides are often adsorbed on the plastron surface in colloid forms, which complex with humic acids from organic matter degradation to further enhance the dark brown color[32]. In summary, the formation of black deposits on the surface of plastrons unearthed at the Taijiasi Site is related to this special burial environment, specifically the lime concretion black soil rich in Fe and Mn.

This study comprehensively utilized various analyses to thoroughly investigate the black deposits on the surface of oracle plastrons unearthed at the Taijiasi Site in Funan, Anhui Province. The results showed that the black discoloration is mainly due to chemical reactions in the burial environment, closely related to the Mn and Fe enrichment, oxidation-reduction reactions, and microbial activities. Mn^{4+} and Fe^{3+} were adsorbed on the oracle plastron surface in colloid forms, complexing with humic acids from organic matter degradation to darken the color. While this study did not conduct microbial detection, the observed elemental transformations are consistent with potential bacterial involvement. This inference is based on the soil type and the observed changes in elemental valence states (Fe^{2+}→Fe^{3+}, Mn^{2+}→Mn^{4+}). Future research could employ metagenomic analysis to identify specific microbial communities and their functional genes. The research findings can provide critical data support for the targeted conservation of oracle plastrons at the Taijiasi site—such as desalination and corrosion inhibition treatments to suppress Mn/Fe oxide deposition—and for studies on the discoloration mechanisms of Shang-Zhou dynasty oracle plastrons in the Jianghuai region.

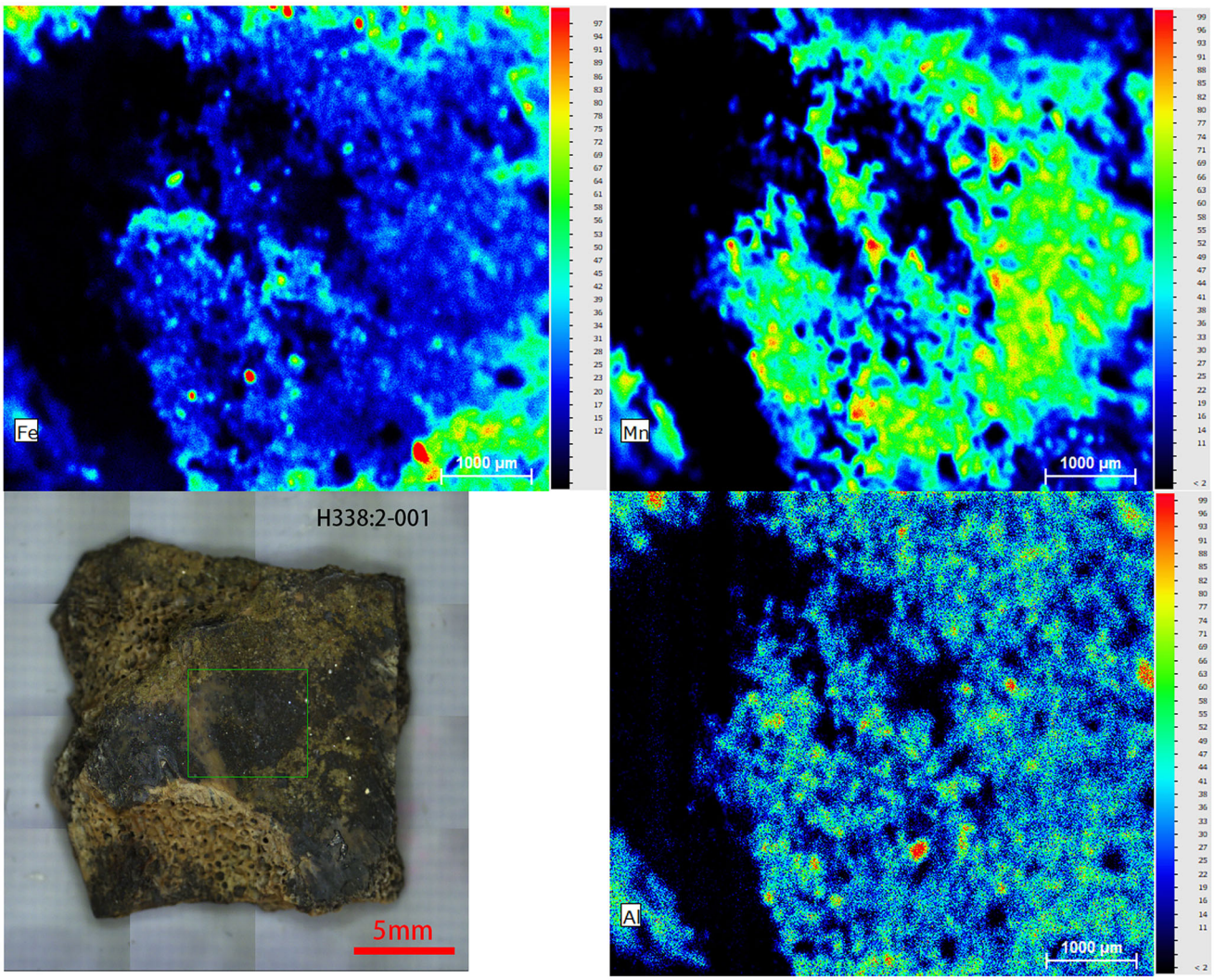

Fig. 9 | Mapping analysis results of Al, Fe, and Mn in the H338:2-001 sample.

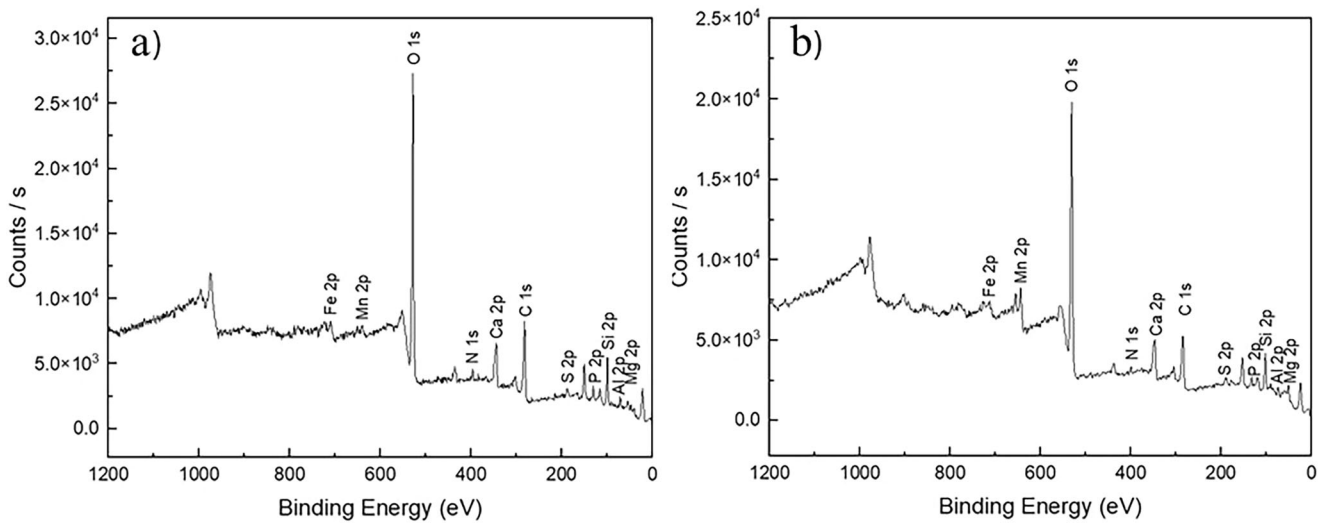

Fig. 10 | XPS spectra of the black deposits on the oracle plastron surface. a Sample H253:2-014; **b** Sample H338:2-001.

Table 3 | Atomic contents of elements on the surface of the oracle plastron samples (at%)

Element	Sample H253:2-014		Sample H338:2-001	
	Peak BE	Atomic%	Peak BE	Atomic%
O1s	531.41	41.61	531.16	42.33
C1s	285.09	28.47	284.73	24.15
Si2p	102.15	14.11	102.03	13.08
Ca2p	347.40	3.99	347.17	4.21
N1s	399.44	3.28	399.87	1.32
S2p	168.00	0.16	163.28	0.07
Mg2p	49.89	1.28	50.71	6.51
Mn2p	642.87	0.34	643.89	3.19
Fe2p	711.53	0.20	712.55	0.12
Al2p	73.81	4.20	73.60	3.51
P2p	133.00	2.36	132.32	1.86

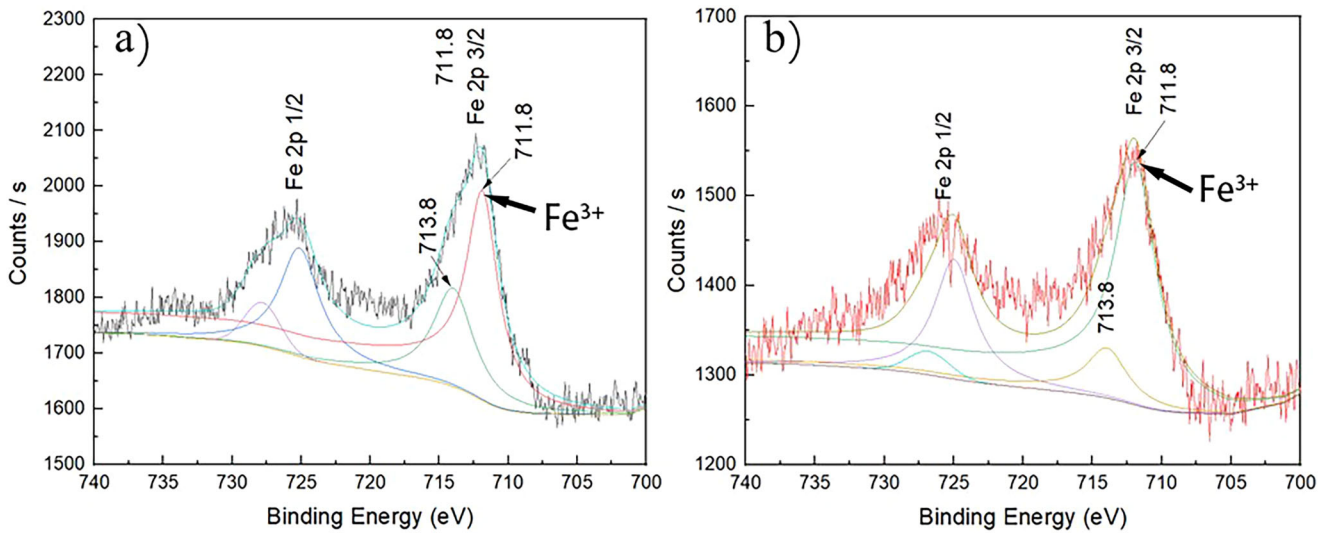

Fig. 11 | Peak deconvolution and curve-fitting of the Fe 2p XPS spectrum. a Sample H253:2-014; **b** Sample H338:2-001.

Data availability

The authors confirm that the data supporting the findings of this study are available within this article.

Received: 12 October 2025; Accepted: 6 January 2026;
Published online: 15 January 2026

References

1. Wang, Y. X. *General Theory of Oracle Bone Studies.* 104–106 (China Social Sciences Press, 1999).
2. Li, X. Q. Basic knowledge about oracle bones. *Hist. Teach.* **7**, 22–24 (1959).
3. Xiong, J., Jiao, Q. J. & Liu, Y. T. Oracle bone studies knowledge graph construction based on multi-source heterogeneous data. *J. Zhejiang Univ.* **47**, 131–141 (2020).
4. Piao, Z. F. *Research on Methods of Divination in the Pre-Qin Period.* 42–44 (Shanghai Chinese Classics Publishing House, 2011).
5. Luo, Z. Y. *A study of Yin Shang Zhen Bu Script*. 3–47 (Shanghai Ancient Books Publishing House, 2013).
6. Shaanxi Zhouyuan Archaeological Team. Early Zhou oracle bone script discovered in Fengchu Village, Qishan, Shaanxi. *Cultural Relics* **30,** 38–43 (1979).
7. Shaanxi Zhouyuan Archaeological Team. Brief report on the excavation of Western Zhou oracle bones in Qijia Village, Fufeng County. *Cultural Relics* **32,** 1–7 (1981).
8. Wang, Y. X. *Discussing Oracle Bones of Western Zhou Dynasty*. 131–139 (China Social Sciences Press, 2023).
9. Fang, H. Archaeological discoveries and researches on the Daxinzhuang Site. *J. Shandong Univ.* **54**, 7–12 (2004).
10. Department of Archaeology, School of History, Wuhan University. Anhui Provincial Institute of Cultural Relics and Archaeology. The excavation of the Taijiasi Site in Funan County, Anhui. *Archaeology* **64**, 603–613 (2018).
11. School of History, Anhui University, Anhui Provincial Institute of Cultural Relics and Archaeology. Excavation of the Dayandun Site in Hefei, Anhui Province. *Southeast Cult.* **38**, 44–55 (2022).
12. Department of Archaeology, School of History, Wuhan University, Anhui Provincial Institute of Cultural Relics and Archaeology. The excavation of the Guduiqiao Site in Fengyang County, Anhui. *Archaeology* **64**, 16–27 (2018).
13. Anhui Provincial Institute of Cultural Relics and Archaeology, Hanshan County Cultural Relics Management Institute. The fourth excavation report of Dachengdun Site in Hanshan County, Anhui Province. *Archaeology* **35**, 103–117 (1989).

14. Zhang, J. Z. & Wang, B. Y. Forensic identification of carbonized human bodies. *Forensic Sci. Technol.* **25**, 36–37 (2000).
15. Zheng, L. P., Wu, X. Z., Jin, P. J. & Chang, Y. P. Discussion of the formation mechanism of a black substance on the surface of fossil bones at the Bailong Cave Site in Yunxi County, Hubei Province. *Acta Anthropol. Sin.* **31**, 364–370 (2012).
16. Ma, D. & Zheng, Y. M. Analysis of iron-sulfur compounds in the southern Song Dynasty shipwreck planks from Huaguang Reef No.1. *Sci. Conserv. Archaeol.* **24**, 84–89 (2012).
17. Shen, D. W., Ge, Q. Y., Yang, M. & Ma, Q. L. The issue of iron-sulfur compounds in the preservation of marine waterlogged wood artifacts. *Sci. Conserv. Archaeol.* **25**, 82–88 (2013).
18. Wang, C. et al. Study on the conservation status of Zhouyuan oracle bones. *Sci. Conserv. Archaeol.* **27**, 14–21 (2015).
19. Liu, R. X. et al. Comparative analysis of the activation mechanism of Ca^{2+} and Fe^{3+} on quartz using infrared spectroscopy and XPS. *Spectrosc. Spectr. Anal.* **40**, 1876–1882 (2020).
20. Biesinger, M. C. et al. Resolving surface chemical states in XPS analysis of first-row transition metals, oxides, and hydroxides: Cr, Mn, Fe, Co, and Ni. *Appl. Surf. Sci.* **257**, 2717–2730 (2011).
21. Chen, J. Y., Feng, B., Zhou, J. L., Jiang, F. G. & Ma, L. G. Study on the effect of roasting temperature on the performance of Mn-based denitrification catalysts based on X-ray photoelectron spectroscopy (XPS) spectra. *Chin. J. Inorg. Anal. Chem.* **15**, 143–149 (2025).
22. Funan County Local Chronicles Compilation Committee. *Funan County Annals*, 64 (Huangshan Publishing House, 1997).
23. Xiong, J. L. Content and distribution of available manganese in soil of Anhui Province. *J. Anhui Agric. Coll.* **17**, 257–262 (1990).
24. Zhang, Z. L. & Luo, X. R. Content and distribution of available copper and iron in soil of Anhui Province. *J. Anhui Agric. Coll.* **17**, 275–279 (1990).
25. Wang, W. J. & Dai, W. H. Study on soil pH and acidic buffering properties in Anhui Province. *Chin. Agric. Sci. Bull.* **28**, 67–72 (2012).
26. Henan Provincial Soil Survey Office. *Henan Soil* 532 (China Agricultural Press, 2004).
27. Huang, C. Y. *Soil Science* 178–185 (China Agricultural Press, 2000).
28. Wu, W. X., Jin, Z. X., Liu, H. D. & Chen, H. C. Study on the speciation analysis of manganese in soil. *Phys. Test. Chem. Anal. Part B Chem. Anal.* **41**, 99–101 (2003).
29. Pan, G. X. Enrichment of transition metals in iron-manganese nodules of Huaibei soil and its environmental geochemical significance. *Chin. Sci. Bull.* **19**, 1505–1507 (1989).
30. Santelli, C. M., Webb, S. M., Dohnalkova, A. C. & Hansel, C. M. Diversity of Mn oxides produced by Mn(II)-oxidizing fungi. *Geochim. et Cosmochim. Acta* **75**, 2762–2776 (2011).
31. Learman, D. R. et al. Coupled biotic–abiotic Mn(II) oxidation pathway mediates the formation and structural evolution of biogenic Mn oxides. *Geochim. et Cosmochim. Acta* **75**, 6048–6063 (2011).
32. Zha, J. et al. Weathering mechanism of red discolorations on Limestone object: a case study from Lingyan Temple, Jinan, Shandong Province, China. *Herit. Sci.* **8**, 54 (2020).

Acknowledgements

This study was funded by the Protection and Restoration Project under the Anhui Provincial Institute of Cultural Relics and Archaeology.

Author contributions

J.Y. analyzed the samples, wrote the main manuscript and reviewed the manuscript; D.G. and Z.Y. both provided useful guidance and helped to review and edit the manuscript; P.J. performed part of the analyses and reviewed the manuscript; X.H. provided the archaeological background and reviewed the manuscript.

Competing interests

The authors declare no competing interests.

Additional information

Correspondence and requests for materials should be addressed to Zhengquan Yao.